Max-Planck-Institut
für Mathematik
in den Naturwissenschaften
Leipzig

Well conditioned boundary integral equations for two-dimensional sound-hard scattering problems in domains with corners

by

Catalin Turc, Jeffrey Ovall, and Akash Anand

Preprint no.: 43 2010

Well conditioned boundary integral equations for two-dimensional sound-hard scattering problems in domains with corners

Akash Anand, Jeff Ovall, Catalin Turc
anand@acm.caltech.edu, jovall@ms.uky.edu, catalin.turc@case.edu

Abstract

We present several well-posed, well-conditioned integral equation formulations for the solution of two-dimensional acoustic scattering problems with Neumann boundary conditions in domains with corners. We call these integral equations Direct Regularized Combined Field Integral Equations (DCFIE-R) formulations because (1) they consist of combinations of direct boundary integral equations of the second-kind and first-kind integral equations which are preconditioned on the left by coercive boundary single-layer operators, and (2) their unknowns are physical quantities, i.e the total field on the boundary of the scatterer. The DCFIE-R equations are shown to be uniquely solvable in appropriate function spaces under certain assumptions on the coupling parameter. Using Calderón's identities and the fact that the unknowns are bounded in the neighborhood of the corners, the integral operators that enter the DCFIE-R formulations are recast in a form that involves integral operators that are expressed by convergent integrals only. The polynomially-graded mesh quadrature introduced by Kress [28] enables the high-order resolution of the weak singularities of the kernels of the integral operators and the singularities in the derivatives of the unknowns in the vicinity of the corners. This approach is shown to lead to an efficient, high-order Nyström method capable of producing solutions of sound-hard scattering problems in domains with corners which require small numbers of Krylov subspace iterations throughout the frequency spectrum. We present a variety of numerical results that support our claims.

Keywords: acoustic scattering, combined-field integral equations, geometric singularities.

1 Introduction

Numerical methods for the solution of acoustic two-dimensional homogeneous scattering problems which are based on integral equation formulations possess certain advantages over their volumetric counterparts. These advantages include not only the obvious reduction in dimensionality that is achieved from posing the scattering problems on the one-dimensional boundary of the scatterers, but also the built-in enforcement of the radiation conditions through choices of outgoing Green's functions. Among the numerical methods that use boundary integral equation formulations, the ones that employ Nyström discretizations are particularly attractive owing to the reduced number of evaluations of Green's functions and the high-order convergence rates that can be achieved. In a nutshell, in the case of one-dimensional smooth boundaries, Nyström methods use global approximations of the unknowns and high-order quadrature rules to integrate weakly singular functions (i.e. singular but integrable) against smooth densities. The case of non-smooth boundaries is more complicated as the densities and/or their derivatives are singular and some of the kernels of the boundary integral operators are no longer weakly singular. These obstacles were overcome in the case of acoustic scattering problems with Dirichlet boundary conditions [19] through the use

of integral equations whose solutions are Hölder continuous, so that polynomially-graded meshes can resolve to high order the singularities in the derivatives of the solutions. In this paper we present (a) several well-posed, well conditioned integral equation formulations for the solution of two-dimensional acoustic scattering problems with sound-hard boundary conditions for domains with corners and (b) a high-order Nyström method to obtain rapidly convergent solutions of these integral equations. To the best of our knowledge, a Nyström method counterpart for the case of Neumann boundary conditions has not been available, partly because of a host of additional difficulties that we outline next.

In order to ensure that the solutions of the integral equation formulations of scattering problems coincide with solutions to the differential formulations of these problems, the former must be uniquely solvable. A wide class of integral equation formulations typically referred to as Combined Field Integral Equations (CFIE) [13, 19] share the unique solvability property. However, CFIE formulations for scattering problems with Neumann-boundary conditions (i.e the sound-hard case) involve hyper-singular operators which resemble, in spirit, differentiation and consequently the eigenvalues of the integral operators that enter these formulations accumulate at infinity. The situation is further complicated by the singular behavior of the solutions of such equations in the presence of corners: depending on the integral equation formulation, the solutions or their derivatives may be singular (unbounded) in a neighborhood of the corner [9, 23, 41, 42].

Our approach to design a high-order Nyström method for the solution of acoustic scattering problems with sound-hard boundary conditions for domains with corners is based on combination of a suitable version of our recently introduced Regularized Combined Field Integral Equations (CFIE-R) [7, 8] and the polynomially-graded mesh quadrature introduced in [28]. To this end, we use direct integral equation formulations that result from applications of the Green's formulas and pose the scattering problem in terms of a physical unknown—that is the total field on the boundary of the scatterer. A key advantage of such formulations is that the total field can be shown to be Hölder continuous (and therefore bounded) in the neighborhood of corners [9, 41].

We obtain Direct Regularized Combined Field Integral Equations (DCFIE-R) by combining compositions of direct integral equations of the first and second kind with suitably defined single layer operators that effectively act as regularizing operators. The regularization strategy is motivated by and directed towards (a) Stabilizing the differentiation effect of the hypersingular operators and (b) Obtaining uniquely solvable integral equations with superior spectral properties. The unique solvability and favorable spectral property in part (b) are established in the framework of Fredholm theory; to the best of our knowledge, we believe that this is the first proof of such properties for integral equations for sound-hard problems in domains with corners. The proof of the Fredholm property of the operators in the DCFIE-R formulations is based on the Fredholm property of boundary integral operators associated to Laplace's equations in Lipschitz domains [17, 25, 40] and the fact that the differences between the acoustic boundary integral operators and their Laplace counterparts are compact [15, 35]. Based on the Fredholm property of the DCFIE-R operators, we show that the unique solvability property is a consequence of a certain coercivity property enjoyed by the regularizing operators that we use. Furthermore, unlike the classical CFIE formulations, our approach bypasses the evaluation of hypersingular operators in the DCFIE-R formulations through the use of Calderón's identities. The methodology that we present in this paper can be extended to the case of sound-hard scattering problems in three dimensions, and the implementation of such strategy is currently underway [3].

The idea of using regularizing operators in the boundary integral equations for acoustic scattering from sound-hard obstacles was originally proposed as a theoretical tool in [12, 19, 37] for the case

of smooth boundaries. Specifically, the scattered fields are represented in the form of combinations of single layer potentials and double layer potentials that act on the regularizing operators, so that the resulting integral operators have bounded spectra. A variety of regularizing/preconditioning strategies of a similar flavor have since been proposed in order to improve the conditioning of boundary integral equations for sound-hard scattering applications [2, 4, 5, 16, 31], yet none of these works addresses directly the case of domains with corners. In the case of Lipschitz domains, a different kind of regularizing technique was introduced in [10, 11] with the goal of obtaining coercive boundary integral formulations for acoustic scattering problems. In contrast with the regularizing techniques introduced in [2, 4, 5, 12, 16, 19, 31, 37], the regularizing operators proposed in [10, 11] act on the single layer operators, and the integral equations that are obtained are first-kind integral equations.

The numerical implementation of the Direct Regularized Combined Field Integral Equations follows the methodology of the Nyström algorithms introduced in [28, 29]. Specifically, our algorithm is based on global trigonometric approximations of the densities, polynomial changes-of-variables, and analytic integration of the most singular part of the kernels of the acoustic integral boundary layer against the Fourier harmonics. The use of the regularizing operators in conjunction with the Calderón's identities bypasses entirely the need to evaluate hypersingular operators. The double-layer operators, on the other hand, whose kernels are singular are recast into a form that involves two parts: one with integrable quantities whose integrals can be evaluated very accurately using the polynomial change of variables and another part which can be evaluated exactly, just as in [28]. We present numerical results for domains with convex and concave corners, various incident fields and frequencies. The DCFIE-R formulations are well-conditioned and their solutions exhibit high-order convergence under Nyström discretizations.

The paper is organized as follows: in Section 2 we introduce and briefly derive our Direct Regularized Combined Field Integral Equations, in Sections 3 we present the numerical algorithm, while numerical results are presented in Section 4.

2 Regularized Combined Field Integral Equations

We are interested in the time-harmonic acoustic scattering problem for a two-dimensional sound-hard obstacle that occupies a bounded domain $D \subset \mathbb{R}^2$, with boundary Γ which is a Lipschitz curve. Given an incident field u^i, defined throughout $\mathbb{R}^2$, we seek a scattered field u^s satisfying the Helmholtz equation outside D,

$$\Delta u^s + k^2 u^s = 0 \text{ in } D^c = \mathbb{R}^2 \setminus \overline{D} \quad , \quad \frac{\partial u^s}{\partial \mathbf{n}} = -\frac{\partial u^i}{\partial \mathbf{n}} \text{ on } \Gamma \ , \tag{1}$$

together with the radiation conditions

$$\lim_{r\to\infty} \sqrt{r}\left(\frac{\partial u^s}{\partial r} - iku^s\right) = 0 \quad , \quad r = |x| \ . \tag{2}$$

In the equations above, the normal derivative operator can be understood in the sense of the Neumann trace, i.e. the operator $\frac{\partial}{\partial \mathbf{n}} : \{u : u \in H^1_{\text{loc}}(D^c),\ \Delta u \in L^2_{\text{loc}}(D^c)\} \to H^{-\frac{1}{2}}(\Gamma)$ which satisfies $\frac{\partial v}{\partial \mathbf{n}} = \nabla v \cdot \mathbf{n}$ for smooth functions $v \in C^\infty(\overline{D^c})$, where $\mathbf{n}$ is the almost everywhere defined unit normal to the curve Γ pointing into D^c. In practice, the given incident field also satisfies the Helmholtz equation as well: $\Delta u^i + k^2 u^i = 0$ in D, D^c or $\mathbb{R}^2$. Existence and uniqueness of the solution

to the scattering problem (1)-(2) has been shown to hold in $\{u : \Delta u \in L^2_{\rm loc}(D^c)\} \cap H^1_{\rm loc}(D^c)$ [34, 35] for boundary data $\frac{\partial u^i}{\partial \mathbf{n}} \in H^{-\frac{1}{2}}(\Gamma)$.

We denote by G_k the outgoing free-space Green's function

$$G_k(\mathbf{z}) = \frac{i}{4} H_0^{(1)}(k|\mathbf{z}|) \ , \tag{3}$$

and by $\mathcal{R}_1, \mathcal{R}_2$ two regularizing operators to be defined later. By construction, any function U of the form

$$U(\mathbf{z}) = \int_\Gamma G_k(\mathbf{z}-\mathbf{y})[\mathcal{R}_1\phi](\mathbf{y})ds(\mathbf{y}) + i\eta \int_\Gamma \frac{\partial G_k(\mathbf{z}-\mathbf{y})}{\partial \mathbf{n}(\mathbf{y})}[\mathcal{R}_2\phi](\mathbf{y})ds(\mathbf{y}) \ , \ \mathbf{z} \notin \Gamma \ , \tag{4}$$

for some suitable density ϕ, satisfies the Helmholtz equation in $\mathbb{R}^2 \setminus \Gamma$ as well as the radiation condition (2). Were we to seek u^s in this form we would see, by taking its Neumann trace and using the standard jump conditions [20], that ϕ must satisfy the boundary integral equation

$$[\mathcal{A}\phi](\mathbf{x}) = -\frac{\partial u^i(\mathbf{x})}{\partial \mathbf{n}(\mathbf{x})} \text{ a.e. on } \Gamma \ , \tag{5}$$

$$[\mathcal{A}\phi](\mathbf{x}) \doteq \left[\left((-I/2 + K_k') \circ \mathcal{R}_1 + i\eta N_k \circ \mathcal{R}_2\right)\phi\right](\mathbf{x}) \ , \tag{6}$$

where $K_k^{'}$ denotes the Neumann trace of the acoustic single-layer operator,

$$(K_k^{'}\phi)(\mathbf{x}) = PV \int_\Gamma \frac{\partial G_k(\mathbf{x}-\mathbf{y})}{\partial \mathbf{n}(\mathbf{x})}\phi(\mathbf{y})ds(\mathbf{y}), \ \mathbf{x} \text{ on } \Gamma \ , \tag{7}$$

and N_k denotes the Neumann trace of the double-layer potential on Γ, whose kernel can be expressed as [19]

$$\frac{\partial^2 G_k(\mathbf{x}-\mathbf{y})}{\partial \mathbf{n}(\mathbf{x})\partial \mathbf{n}(\mathbf{y})} = -\frac{\partial^2 G_k(\mathbf{x}-\mathbf{y})}{\partial \mathbf{t}(\mathbf{x})\partial \mathbf{t}(\mathbf{y})} + k^2 G_k(\mathbf{x}-\mathbf{y})\mathbf{n}(\mathbf{x}) \cdot \mathbf{n}(\mathbf{y}) \ . \tag{8}$$

Here and elsewhere $\partial/\partial \mathbf{t}$ denotes the tangential derivative on Γ, where $\mathbf{t} = (-n_2, n_1)$ for $\mathbf{n} = (n_1, n_2)$. We note that the classical CFIE [13] amounts to taking $\mathcal{R}_i = I, \ i = 1, 2$ in equations (5). We remark that all integral equations in Section 2 hold a.e. on Γ, yet we will omit mentioning this for each occurence.

Alternatively, assuming that the incident field satisfies $u^i \in C^\infty(\bar{D})$ and $\Delta u^i + k^2 u^i = 0$ in D, and taking into account the regularity of the radiative solution u^s to the Helmholtz equation (1), i.e. $u^s \in H^1_{\rm loc}(D^c)$ and $\Delta u^s \in L^2_{\rm loc}(D^c)$, the application of Green's formulas [20, 22, 34] yields

$$u^s(\mathbf{z}) = \int_\Gamma \left(\frac{\partial G_k(\mathbf{z}-\mathbf{y})}{\partial \mathbf{n}(\mathbf{y})} u^s(\mathbf{y}) - G_k(\mathbf{z}-\mathbf{y}) \frac{\partial u^s(\mathbf{y})}{\partial \mathbf{n}(\mathbf{y})} \right) ds(\mathbf{y}) \ , \tag{9}$$

$$0 = \int_\Gamma \left(\frac{\partial G_k(\mathbf{z}-\mathbf{y})}{\partial \mathbf{n}(\mathbf{y})} u^i(\mathbf{y}) - G_k(\mathbf{z}-\mathbf{y}) \frac{\partial u^i(\mathbf{y})}{\partial \mathbf{n}(\mathbf{y})} \right) ds(\mathbf{y}) \ , \tag{10}$$

for $z \in \mathbb{R}^2 \setminus \overline{D}$. Combining (9) and (10), and recalling the boundary condition in (1), we obtain

$$u^s(\mathbf{z}) = \int_\Gamma \frac{\partial G_k(\mathbf{z}-\mathbf{y})}{\partial \mathbf{n}(\mathbf{y})} u(\mathbf{y})ds(\mathbf{y}) \ , \tag{11}$$

where $u = u|_\Gamma = u^s + u^i$ is the Dirichlet trace of the total field u on Γ. Taking the Dirichlet and Neumann traces of (11), together with the standard jump-relations [19, 20, 34], we obtain the boundary integral equations

$$\frac{u(\mathbf{x})}{2} - (K_k\ u)(\mathbf{x}) = u^i(\mathbf{x}) \ \text{ and } \ -(N_k\ u)(\mathbf{x}) = \frac{\partial u^i(\mathbf{x})}{\partial \mathbf{n}(\mathbf{x})} \ \text{ on } \Gamma\ , \tag{12}$$

where K_k denotes double-layer potential on Γ defined as a Cauchy Principal Value integral:

$$(K_k\phi)(\mathbf{x}) = PV \int_\Gamma \frac{\partial G_k(\mathbf{x}-\mathbf{y})}{\partial \mathbf{n}(\mathbf{y})}\phi(\mathbf{y}) ds(\mathbf{y}) \text{ on } \Gamma\ . \tag{13}$$

Taking a cue from the derivation of the formulations (5), we combine regularized versions of the equations in (12), resulting in

$$[\mathcal{A}'u](\mathbf{x}) = [\mathcal{R}_1 u^i](\mathbf{x}) + i\eta \left[\mathcal{R}_2 \frac{\partial u^i}{\partial \mathbf{n}}\right](\mathbf{x}) \ \text{ on } \Gamma\ , \tag{14}$$

$$[\mathcal{A}'u](\mathbf{x}) \doteq \left[(\mathcal{R}_1 \circ (I/2 - K_k) - i\eta \mathcal{R}_2 \circ N_k)\, u\right](\mathbf{x})\ . \tag{15}$$

We are primarily interested in the DCFIE-R (14) in the present work, but for certain choices of regularizing operators $\mathcal{R}_1, \mathcal{R}_2$ the unique solvability of both types of integral equations is linked via duality arguments, which is why we have chosen the suggestive notation $\mathcal{A}'$—$\mathcal{A}$ and $-\mathcal{A}'$ are adjoint operators with respect to the (real) L^2-inner-product.

2.1 The unique solvability of ICFIE-R and DCFIE-R

The unique solvability of the integral equations (5) for suitable choices of the operators $\mathcal{R}_i$ is settled via Fredholm alternative type of arguments [8, 13] typically in the functional space $H^{-\frac{1}{2}}(\Gamma)$, at least in the case of smooth boundaries Γ. A key ingredient in the proof of the Fredholm property of the integral operators in equations (5) is the compactness of the double layer operators $K_k^{'}$. Such an argument is not available in the case of Lipschitz curves Γ, yet by relying on the techniques developed in a series of papers [17, 25, 40] we will prove the Fredholm property of the aforementioned operators in suitable functional spaces for certain choices of the operators $\mathcal{R}_i$. We note that in the case of Dirichlet boundary conditions for the Helmholtz equation, the Fredholm property of the CFIE operators, and hence the unique solvability and well-posedness of CFIE equations, was proved to hold in $H^{s-\frac{1}{2}}(\Gamma)$, $|s| \leq \frac{1}{2}$ using the same techniques mentioned above [15, 35]. Indeed, in the case of Dirichlet boundary conditions, a combined field representation of the type (4) with $\mathcal{R}_1 = I$ and $\mathcal{R}_2 = (S_0)^2$ was employed in [35], whereas the classical $\mathcal{R}_i = I$ was used in [15].

The classical results about the regularity properties of $K_0^{'}$ [17, 25, 40] and compactness arguments yield that $K_k^{'}$ is a bounded operator on $L^2(\Gamma)$ [35]. More generally, it can be shown [20, 24] that $K_k^{'} : H^{-\frac{1}{2}+s}(\Gamma) \to H^{-\frac{1}{2}+s}(\Gamma)$ is a continuous operator for $|s| \leq \frac{1}{2}$. Furthermore, using equation (8), the operator N_k can be expressed in terms of a Cauchy Principal Value integral [20]. In particular, for a density $\phi \in H^1(\Gamma)$ (in fact it suffices that $\phi \in L^2_1(\Gamma) = \{\psi \in L^2(\Gamma) :\ \partial\psi/\partial\mathbf{t} \in L^2(\Gamma)\}$—a space introduced in [40]), the operator N_k can be expressed in terms of a Hilbert transform

$$(N_k\phi)(\mathbf{x}) = k^2 \int_\Gamma G_k(\mathbf{x}-\mathbf{y})(\mathbf{n}(\mathbf{x})\cdot\mathbf{n}(\mathbf{y}))\phi(\mathbf{y}) ds(\mathbf{y}) + \text{PV} \int_\Gamma \frac{\partial G_k(\mathbf{x}-\mathbf{y})}{\partial \mathbf{t}(\mathbf{x})} \frac{\partial \phi(\mathbf{y})}{\partial \mathbf{t}(\mathbf{y})}\, ds(\mathbf{y})\ , \tag{16}$$

as thus it can be seen to be a bounded operator from $H^1(\Gamma)$ (or $L^2_1(\Gamma)$) into $L^2(\Gamma)$. More generally, $N_k : H^{\frac{1}{2}+s}(\Gamma) \to H^{-\frac{1}{2}+s}(\Gamma)$ is a continuous operator for $|s| \leq \frac{1}{2}$ [20, 25].

We will show that for certain choices of the regularizing operator $\mathcal{R}_i$, $i = 1, 2$, equations (5) are uniquely solvable in $L^2(\Gamma)$ (actually the invertibility property holds in all of the spaces $H^{s-\frac{1}{2}}(\Gamma)$ for $|s| \leq \frac{1}{2}$). We note that for most applications of interest the incident fields are such that u^i is smooth in a neighborhood of Γ and thus $\frac{\partial u^i}{\partial \mathbf{n}} \in L^2(\Gamma)$. The regularizing operators $\mathcal{R}_i$ that we use are defined as

$$(\mathcal{R}\phi)(\mathbf{x}) = (S_0^d\phi)(\mathbf{x}) = \int_\Gamma G_0\left(\frac{\mathbf{x}-\mathbf{y}}{d}\right)\phi(\mathbf{y})ds(\mathbf{y}),\ \mathbf{x} \text{ on } \Gamma \tag{17}$$

where $G_0(\mathbf{z}) = -\frac{1}{2\pi}\log|\mathbf{z}|$ is the free-space Green's function for the Laplace's equation and d is such that $\mathrm{diam}(D) < d$ (note that it would actually suffice to take $d > \mathrm{Cap}(\Gamma)$, where $\mathrm{Cap}(\Gamma)$ is the capacitance of Γ [34]). The operators S_0^d can be written in terms of single-layer operators S_0 corresponding to the Laplace's equation

$$(S_0^d\phi)(\mathbf{x}) = (S_0\phi)(\mathbf{x}) + \frac{\log d}{2\pi}\int_\Gamma \phi(\mathbf{y})ds(\mathbf{y}). \tag{18}$$

Using the results in [20, 25] it can be shown that $S_0^d : H^{-\frac{1}{2}+s}(\Gamma) \to H^{\frac{1}{2}+s}(\Gamma)$ is a continuous operator for $|s| \leq \frac{1}{2}$. Using the regularizing operators $\mathcal{R}$ defined above, the following result holds true:

Theorem 2.1 *For following choices of regularizing operators and real, non-zero coupling parameters η, the operator $\mathcal{A}$ is invertible on $L^2(\Gamma)$:*

1) $\mathcal{R}_1 = I,\ \mathcal{R}_2 = (S_0^d)^2$;

2) $\mathcal{R}_1 = \mathcal{R}_2 = S_0^d$;

3) $\mathcal{R}_1 = I,\ \mathcal{R}_2 = S_0^d,\ 0 < |\eta| < C < 1$, *where* $C = C(\Gamma)$.

We refer to the ICFIE formulations (5) coming from these choices as ICFIE-R(0,2), ICFIE-R(1,1) *and* ICFIE-R(0,1), *respectively.*

Proof. We will first establish that $\mathcal{A}$ is Fredholm for the choices (1)–(3) above. To this end, we use Calderón's identity [14, 20, 22]

$$N_0 \circ S_0 = -\frac{I}{4} + (K_0')^2 \tag{19}$$

and equation (18) together with the fact that [30]

$$\int_\Gamma\int_\Gamma \frac{\partial^2 G_0(\mathbf{x}-\mathbf{y})}{\partial\mathbf{n}(\mathbf{x})\partial\mathbf{n}(\mathbf{y})}\phi(\mathbf{y})ds(\mathbf{y})ds(\mathbf{x}) = 0 \tag{20}$$

to express $N_k \circ S_0^d$ as

$$N_k \circ S_0^d = (N_k - N_0)\circ S_0^d - \frac{I}{4} + (K_0')^2\ . \tag{21}$$

In order to prove the Fredholmness of $\mathcal{A}$ we will use the following two facts:

- $K_k' - K_0'$, S_0^d and $(N_k - N_0)\circ S_0^d$ are compact operators in $L^2(\Gamma)$ [22, 35];

- $I/2 \pm K_0^{'}$ are Fredholm operators of index 0 on $L^2(\Gamma)$ [40].

In case 1) we have

$$\mathcal{A} = (K_0^{'} - I/2) + (K_k^{'} - K_0^{'}) + i\eta[(N_k - N_0) \circ S_0^d] \circ S_0^d - i\eta(I/2 + K_0^{'}) \circ (I/2 - K_0^{'}) \circ S_0^d \quad (22)$$

which can be seen to be a compact perturbation of the Fredholm operator $K_0^{'} - I/2$ on $L^2(\Gamma)$. Thus, $\mathcal{A}$ is Fredholm in $L^2(\Gamma)$. In case 2) we have

$$\mathcal{A} = (K_0^{'} - I/2) \circ S_0^d + (K_k^{'} - K_0^{'}) \circ S_0^d + i\eta[(N_k - N_0) \circ S_0^d] - i\eta(I/2 + K_0^{'}) \circ (I/2 - K_0^{'}). \quad (23)$$

The first three operators in the right hand side of equation (23) are compact operators in $L^2(\Gamma)$, while the latter operator is a composition of Fredholm operators and thus Fredholm. Again, $\mathcal{A}$ is Fredholm on $L^2(\Gamma)$. Finally, in case 3), we have

$$\mathcal{A} = (K_k^{'} - K_0^{'}) + i\eta[(N_k - N_0) \circ S_0^d] - (1 + i\eta/2)\left(I + \frac{i\eta}{1 + i\eta/2} K_0^{'}\right) \circ (I/2 - K_0^{'}). \quad (24)$$

The first two operators in the right-hand side of equation (24) are compact on $L^2(\Gamma)$. On the other hand, the operator $I/2 - K_0^{'}$ is Fredholm cf. (b) above, while for $|\eta| < ||K_0^{'}||_2^{-1}$ the operator $I + \frac{i\eta}{1+i\eta/2} K_0^{'}$ is invertible on $L^2(\Gamma)$. Thus, since the latter operators commute, their composition is Fredholm and consequently $\mathcal{A}$ is yet again Fredholm for option 3). We note that $||K_0^{'}||_2$ depends on the curve Γ alone, and bounds on its size were provided in [17].

We will now show that the null-space of $\mathcal{A}$ is trivial for the choices $\mathcal{R}_i$ as presented in cases 1)–3). Indeed, for a density ϕ in the null-space of $\mathcal{A}$ we define U^+ for $\mathbf{z} \in D^c$ and U^- for $\mathbf{z} \in D$ via equation (4). Since U^+ is a radiative Helmholtz solution in D^c satisfying $\partial U^+/\partial \mathbf{n} = \mathcal{A}\phi = 0$ on Γ, we must have $U^+ = 0$ in D^c, and hence on Γ. The jump relations for the Dirichlet and Neumann traces of U^+ and U^-, together with the fact that $\partial U^+/\partial \mathbf{n} = U^+ = 0$ on Γ, combine to give us

$$-U_- = i\eta\ \mathcal{R}_2\phi \ \text{ and } \ \frac{\partial U^-}{\partial \mathbf{n}} = \mathcal{R}_1\phi \ \text{ on } \Gamma\ .$$

Using Green's identities we obtain

$$i\eta \int_\Gamma (\mathcal{R}_1\phi)\overline{\mathcal{R}_2\phi} ds = \int_\Gamma \bar{U}^- \frac{\partial U^-}{\partial \mathbf{n}} ds = \int_D (|\nabla U_-|^2 - k^2|U^-|^2) dx. \quad (25)$$

Note that the choices 1) and 2) amount to $i\eta||S_0^d\phi||_2^2 \in \mathbb{R}$, and thus $S_0^d\phi = 0$. In case 3), the kernel of the operator S_0^d is positive owing to the fact that $|\mathbf{x} - \mathbf{y}| < d$ on $\Gamma \times \Gamma$, and hence the operator S_0^d is coercive [20, 34, 36] — $\int_\Gamma (S_0^d\phi)\bar{\phi} ds\ \geq 0$ for all ϕ in $H^{-\frac{1}{2}}(\Gamma) \supset L^2(\Gamma)$, with equality if and only if $\phi = 0$. Clearly, since $\eta \in \mathbb{R}$ and $\eta \neq 0$, equation (25) implies that $\int_\Gamma (S_0^d\phi)\bar{\phi} ds\ = 0$ for all the choices 1)–3), and therefore $\phi = 0$. Consequently, $\mathcal{A}$ is injective and thus the integral equations (5) are uniquely solvable on $L^2(\Gamma)$. ∎

Remark 2.2 *Similar arguments as in the proof of Theorem 2.1 yield that the operators in the left-hand side of (5) are invertible in $H^{s-\frac{1}{2}}(\Gamma)$ for all $|s| \leq \frac{1}{2}$. Indeed, the proof relies on the fact that $\mathcal{A}$ is Fredholm of index 0 as an operator from $H^{s-\frac{1}{2}}(\Gamma)$ to itself for $|s| \leq \frac{1}{2}$. The latter statement is a consequence of compactness arguments similar to those used in the proof of Theorem 2.1 and the fact that $I/2 \pm K_0^{'}$ is Fredholm of index zero in $H^{s-\frac{1}{2}}(\Gamma)$ for $|s| \leq \frac{1}{2}$ [15, 40]. The injectivity*

of the operator $\mathcal{A}$ in $H^{s-\frac{1}{2}}(\Gamma)$ for $|s| \leq \frac{1}{2}$ can be shown using classical arguments. Indeed, since $L^2(\Gamma)$ is dense in $H^{-1}(\Gamma)$ and the operators $\mathcal{A}$ are Fredholm of index 0 in the spaces $H^{s-\frac{1}{2}}(\Gamma)$ for all $|s| \leq \frac{1}{2}$, a standard argument about Fredholm operators [38] gives that the null-space of $\mathcal{A}$, as an operator on $H^{-1}(\Gamma)$, is actually included in $L^2(\Gamma)$. Since the argument in Theorem 2.1 shows that the null-space of $\mathcal{A}$ is trivial in $L^2(\Gamma)$, it follows that the operator $\mathcal{A}$ is injective and thus invertible on $H^{-1}(\Gamma)$, and by interpolation is invertible in all of the spaces $H^{s-\frac{1}{2}}(\Gamma)$ for $|s| \leq \frac{1}{2}$.

Remark 2.3 *The results of Theorem 2.1 remain valid if the operators S_0^d are replaced by $S_{iK},\ K > 0$, that is single layer operators corresponding to purely imaginary wavenumbers in the definition of the operators $\mathcal{R}_j,\ j = 1, 2$ in cases (1)–(3). Indeed, using Calderon's identities (21) for S_{iK} and the coercivity of S_{iK} in $H^{-\frac{1}{2}}(\Gamma)$, the result follows along the same lines as in the proof of Theorem 2.1.*

The following result concerns the unique solvability of equations (14) in a wide range of Sobolev spaces. Indeed, for the same choice of the regularizing operators $\mathcal{R}_i$, $i = 1, 2$ as in Theorem 2.1 the following result, holds true:

Theorem 2.4 *For the following choices of regularizing operators and real, non-zero coupling parameters η, the operator $\mathcal{A}'$ is invertible on $H^{s+\frac{1}{2}}(\Gamma)$ for $|s| \leq \frac{1}{2}$:*

1. $\mathcal{R}_1 = I,\ \mathcal{R}_2 = (S_0^d)^2$;
2. $\mathcal{R}_1 = \mathcal{R}_2 = S_0^d$;
3. $\mathcal{R}_1 = I,\ \mathcal{R}_2 = S_0^d,\ 0 < |\eta| < C < 1$, *where* $C = C(\Gamma, s)$.

We refer to the DCFIE formulations (14) coming from these choices as DCFIE-R(0,2), DCFIE-R(1,1) *and* DCFIE-R(0,1), *respectively.*

Proof. The result follows from Theorem 2.1 and Remark 2.2 via a duality argument. Indeed, for the choices of $\mathcal{R}_i$ in cases (1)–(3), $\mathcal{A}$ and $\mathcal{A}'$ are, up to sign, dual/adjoint operators in the sense of the natural duality between the spaces $H^{s-\frac{1}{2}}(\Gamma)$ and the spaces $H^{-s+\frac{1}{2}}(\Gamma)$ for $|s| \leq \frac{1}{2}$. ■

The following result is a consequence of Theorem 2.4

Corollary 2.5 *Suppose that the Dirichlet and Neumann traces on Γ of the given incident field u^i satisfy: $\frac{\partial u^i}{\partial \mathbf{n}} \in H^{s-\frac{1}{2}}(\Gamma)$ and $u^i \in H^{s+\frac{1}{2}}(\Gamma)$ for some $|s| \leq \frac{1}{2}$. Then the equation (14) has a unique solution u in $H^{s+\frac{1}{2}}(\Gamma)$ for the same choice of the regularizing operators $\mathcal{R}_i$ as in Theorem 2.4. Furthermore, $(\mathcal{A}')^{-1}$ is a continuous operator on $H^{s+\frac{1}{2}}(\Gamma)$.*

Proof. From the regularity theory of the solutions of the Neumann problem (1) it follows that the Dirichlet trace $u \in H^{s+\frac{1}{2}}(\Gamma)$ and that u satisfies equation (14) as a consequence of Green's identities. ■

Remark 2.6 *Using regularizing operators $\mathcal{R}_i = S_{iK},\ K > 0$ instead of S_0^d in the definition of formulations (14), we will call the ensuing integral equations DCFIE-RC. Based on the results in Remark 2.3, the results in Theorem 2.4 hold for the formulations DCFIE-RC(0,1), DCFIE-RC(1,1), and DCFIE-RC(0,2).*

2.2 Remarks on the regularity of the solutions of ICFIE-R and DCFIE-R

We note that the solution of (14) (DCFIE-R) is the total field on the boundary, $u = u^i + u^s$, for any of the choices of regularizing operators given in Theorem 2.4. If we assume that the Neumann data $\frac{\partial u^i}{\partial \mathbf{n}}$ is in $H^{\varepsilon-\frac{1}{2}}(\Gamma)$, then the scattered field u^s, which is the solution to (1), has the following classical regularity property $u^s \in \{u : \Delta u \in L^2_{\rm loc}(D^c),\ u \in H^1_{\rm loc}(D^c)\}$ [34]. Using the Gagliardo trace results in [20] we get that the Dirichlet trace of the total field $u = u^s + u^i$ on Γ belongs to $H^{\varepsilon+\frac{1}{2}}(\Gamma)$—such functions are at least bounded. We can make much stronger statements about the regularity of u on Γ for common classes of incident fields u^i:

- Plane-wave: $u^i(\mathbf{z}) = e^{ik\mathbf{z}\cdot\mathbf{d}}$, where $\mathbf{d}$ is a constant unit vector;
- Point-source: $u^i(\mathbf{z}) = H_0^{(1)}(k|\mathbf{z}-\mathbf{z}_0|)$, where $\mathbf{z}_0 \in D^c$.

Such incident fields satisfy Helmholtz equation within D and are smooth in a neighborhood of Γ. In particular, if Γ is piecewise smooth, then $\frac{\partial u^i}{\partial \mathbf{n}}$ is smooth, except for jump-discontinuities at the corners of Γ. Using results of Wigley [41, Theorem 3.3], we describe the leading asymptotic behavior of u in neighborhoods of the corners, which is the same as the leading asymptotic behavior of u^s.

Theorem 2.7 *Suppose that D has m separated corners at the points x_j, and that the measure of the angle at x_j (measured in D^c) is $\beta_j\pi > 0$. Let $r_j = \mathrm{dist}(x, x_j)$. Then there is a constant κ_j such that $u(x) - u(x_j) = \pm\kappa_j r_j^{1/\beta_j} + \mathcal{O}(r_j)$ as $x \to x_j$ along Γ. The sign on κ_j is determined by the side of x_j from which x approaches.*

The situation is not as favorable for the solution ϕ of (5) (ICFIE-R), where it is often the case that ϕ is unbounded near the corners, as will be argued below. Expressed as the combined potential (4), the Dirichlet and Neumann traces of the solution u^s of (1) satisfy

$$u^s = [S_k \circ \mathcal{R}_1 + i\eta(I/2 + K_k) \circ \mathcal{R}_2]\,\phi \qquad \text{on } \Gamma\ , \tag{26}$$

$$\frac{\partial u^s}{\partial \mathbf{n}} = \left[(-I/2 + K_k') \circ \mathcal{R}_1 + i\eta N_k \circ \mathcal{R}_2\right]\phi = -\frac{\partial u^i}{\partial \mathbf{n}} \qquad \text{on } \Gamma\ . \tag{27}$$

Defining a function v^i in D by the same combined potential, we find that its Dirichlet and Neumann traces are

$$v^i = [S_k \circ \mathcal{R}_1 + i\eta(-I/2 + K_k) \circ \mathcal{R}_2]\,\phi = u^s - i\eta\mathcal{R}_2\phi \qquad \text{on } \Gamma\ , \tag{28}$$

$$\frac{\partial v^i}{\partial \mathbf{n}} = \left[(I/2 + K_k') \circ \mathcal{R}_1 + i\eta N_k \circ \mathcal{R}_2\right]\phi = \mathcal{R}_1\phi - \frac{\partial u^i}{\partial \mathbf{n}} \qquad \text{on } \Gamma\ . \tag{29}$$

Assuming that $\mathcal{R}_2 = \mathcal{R}_1$, we have that $\mathcal{R}_1\phi = \frac{\partial v^i}{\partial \mathbf{n}} + \frac{\partial u^i}{\partial \mathbf{n}}$, where v^i satisfies the Helmholtz equation in D together with the impedance boundary condition $v^i + i\eta\frac{\partial v^i}{\partial \mathbf{n}} = u^s - i\eta\frac{\partial u^i}{\partial \mathbf{n}}$. The same sort of argumentation using [41, Theorem 3.3], albeit more involved (cf. [9]), can be used to show that the leading asymptotic behavior of $\frac{\partial v^i}{\partial \mathbf{n}}$, and hence of $\mathcal{R}_1\phi$, is $\frac{\partial v^i(x)}{\partial \mathbf{n}} \sim \mathcal{R}_1\phi \sim r_j^{\sigma_j}$ near x_j, where $\sigma_j = \min\{1/\beta_j, 1/(2-\beta_j)\} - 1 < 0$. In other words, $\mathcal{R}_1\phi$ is generally unbounded near corners. If $\mathcal{R}_1 = \mathcal{R}_2 = I$ (no regularizing), or $\mathcal{R}_1 = \mathcal{R}_2 = S_0^d$ (ICFIE-R(1,1)), this implies that ϕ is generally unbounded near the corners. This sort of singular behavior for problems with corners is well-documented, see for example [6, 9, 21, 23, 26, 27, 33, 41, 42].

3 Nyström discretization

We succinctly present a high-order Nyström method for the discretization of the integral equations (14), with $\mathcal{A}'$ recast according to formula (33). Without loss of generality, we will assume that D has a single corner at x_0 whose aperture measured inside D is γ_0, and that $\Gamma \setminus \{x_0\}$ is C^2 and piecewise analytic. Assuming that the incident fields u^i are regular enough in a neighborhood of the curve Γ so that $\frac{\partial u^i}{\partial \mathbf{n}} \in H^{-\frac{1}{2}+\epsilon}(\Gamma)$ for $\epsilon > 0$, then the results of Theorem 2.5 apply, and we can consider the integral equation (14) whose solution $u \in H^{\frac{1}{2}+\epsilon}(\Gamma)$. In this case, it follows from Sobolev embedding results that the Dirichlet trace u on Γ of the total field is actually Hölder continuous. This will enable us to express $\mathcal{A}'$ in terms of integral operators that involve integrable quantities only. Indeed, following [19], we can employ the operator $\tilde{K}_0$ defined for continuous functions ψ as

$$(\tilde{K}_0\psi)(\mathbf{x}) = \int_\Gamma \frac{\partial G_0(\mathbf{x}-\mathbf{y})}{\partial \mathbf{n}(\mathbf{y})}[\psi(\mathbf{y}) - \psi(x_0)]ds(\mathbf{y}) \tag{30}$$

so that we can write the first part of equation (12) for all points $\mathbf{x}$ on Γ:

$$\frac{1}{2}[u(\mathbf{x}) + u(x_0)] - (K_k - K_0)(u)(\mathbf{x}) - (\tilde{K}_0 u)(\mathbf{x}) = u^i(\mathbf{x}),\ \mathbf{x} \in \Gamma. \tag{31}$$

Furthermore, using equation (31) together with the Calderón's identities

$$S_0^d \circ N_k = S_0^d \circ (N_k - N_0) - \frac{I}{4} + (K_0)^2 \tag{32}$$

we can express the operator $\mathcal{A}'$ in the formulation DCFIE-R(0,1) in the following manner

$$\begin{aligned}(\mathcal{A}'u)(\mathbf{x}) &= \frac{1}{2}[u(\mathbf{x}) + u(x_0)] - ([(K_k - K_0) + \tilde{K}_0]u)(\mathbf{x}) \\ &+ \frac{i\eta}{4}[u(\mathbf{x}) - u(x_0)] - i\eta([S_0^d \circ (N_k - N_0) + (\tilde{K}_0)^2]u)(\mathbf{x}) \\ &+ \frac{i\eta}{2}[\tilde{K}_0 u](x_0).\end{aligned} \tag{33}$$

We make a couple of remarks about equation (33): first, the equation holds for all points $\mathbf{x}$ on Γ and not almost everywhere, and second, owing to the Hölder continuity of u, the operators $K_k - K_0$, $\tilde{K}_0$, and $N_k - N_0$ are defined as a convergent integrals. Though we do not do so explicitly here, it is clear how to express $\mathcal{A}'$ in the above fashion for DCFIE-R(0,2) and DCFIE-R(1,1) as well. We also give the decomposition of $\mathcal{A}'$ for the "complex version" DCFIE-RC(0,1)

$$\begin{aligned}(\mathcal{A}'u)(\mathbf{x}) &= \frac{1}{2}[u(\mathbf{x}) + u(x_0)] - ([(K_k - K_0) + \tilde{K}_0]u)(\mathbf{x}) + \frac{i\eta}{4}u(x_0)\,((K_{iK} - K_0)1)(\mathbf{x}) \\ &+ \frac{i\eta}{4}[u(\mathbf{x}) - u(x_0)] + \frac{i\eta}{2}([(K_{iK} - K_0) + \tilde{K}_0]u)(x_0) \\ &- i\eta([S_{iK} \circ (N_k - N_{iK}) + ((K_{iK} - K_0) + \tilde{K}_0)^2]u)(\mathbf{x})\ ,\end{aligned} \tag{34}$$

with similar decompositions for the formulations DCFIE-RC(1,1) and DCFIE-R(0,2). The remarks concerning equation (33) are in place for equation (34).

Our approach uses both a high-order treatment of the singularities of the integrable kernels of the integral operators in (33) along the lines of [29], as well as a resolution of the singular nature of the higher-order derivatives of total field u on the curve Γ in the neighborhood of the corner x_0 via the graded meshes introduced in [28]. Many of the formulas and derivations presented here can be found in, or constructed from, those references, but we collect them here for the sake of completeness.

3.1 Parameterization of the Operators

Assuming that the boundary curve $\Gamma \setminus \{x_0\}$ is piecewise analytic and given by the 2π periodic parametrization $x(t) = (x_1(t), x_2(t))$ so that $|x'(t)| \geq s_0 > 0$ and $x(0) = x(2\pi) = x_0$, we start by expressing in parametric form the kernels of the integral operators in (33). Following the notation given above, we define $\mathbf{r} = \mathbf{r}(t,\tau) = x(t) - x(\tau)$ and $r = r(t,\tau) = |\mathbf{r}(t,\tau)|$. For an arbitrary Hölder continuous density $\phi(x)$, $x \in \Gamma$, we define $\psi(t) = \phi(x(t))$. We consider only the case of non-zero wave numbers, $k \neq 0$, and will look at parametric forms of each of the key integral operators appearing in $\mathcal{A}'$ for CFIE-R(0,1). Similar expressions appear for the other real or complex regularizing pairs $(\mathcal{R}_1, \mathcal{R}_2)$, but we will not give them here for sake of brevity.

In parametric form, $[S_0^d(\phi)](x(t))$ can be expressed as

$$[S_0^d(\phi)](x(t)) = \int_0^{2\pi} \left(\frac{\log d}{2\pi} - \frac{\log r^2}{4\pi} \right) |x'(\tau)| \psi(\tau)\, d\tau = \int_0^{2\pi} M_0(t,\tau)\psi(\tau)\, d\tau \tag{35}$$

$$= \int_0^{2\pi} \left(M_{01}(t,\tau) \log r^2 + M_{02}(t,\tau) \right) \psi(\tau)\, d\tau \ . \tag{36}$$

It is clear that $M_{01}(t,t) = -\frac{|x'(t)|}{4\pi}$ and $M_{02}(t,t) = \frac{|x'(t)| \log d}{2\pi}$. Similarly, we have

$$[\tilde{K}_0(\phi)](x(t)) = \int_0^{2\pi} \frac{\mathbf{r} \cdot \nu(\tau)}{2\pi\, r^2} \left(\psi(\tau) - \psi(0) \right) d\tau = \int_0^{2\pi} H_0(t,\tau) \left(\psi(\tau) - \psi(0) \right) d\tau \ . \tag{37}$$

Here and below, $\nu(\tau) = \mathbf{n}(x(\tau))|x'(\tau)| = (-x_2'(\tau), x_1'(\tau))$. Though it may not be immediately apparent, H_0 is smooth on $(0, 2\pi) \times (0, 2\pi)$, with $H_0(t,t) = \frac{x''(t) \cdot \nu(t)}{4\pi |x'(t)|^2}$ for $t \neq 0, 2\pi$ [28]. However, $H_0(t,\tau) \sim 1/r$ as $t \to 0$ and $\tau \to 2\pi$, or as $t \to 2\pi$ and $\tau \to 0$, which is why we integrate against $\psi(\tau) - \psi(0)$, because it vanishes to some (fractional) power at $\tau = 0, 2\pi$, so the product is uniformly integrable for each t.

Let $F(z) = \frac{i}{4} H_0^{(1)}(k\, z) + \frac{\log z}{2\pi}$. We have [1]

$$F(z) = \left(\frac{i}{4} - \frac{\gamma + \log(k/2)}{2\pi} \right) J_0(kz) + \frac{1}{2\pi} \sum_{m=1}^{\infty} \frac{(-1)^m h_m}{(m!)^2} \left(\frac{kz}{2} \right)^{2m} + \frac{1 - J_0(kz)}{4\pi} \log(z^2) \ , \tag{38}$$

where $h_m = \sum_{j=1}^{m} j^{-1}$ is the m^{th} harmonic number, and $\gamma \approx 0.5772156649$ is the Euler-Mascheroni constant. For the difference of double-layer operators, we have

$$[(K_k - K_0)\phi](x(t)) = \int_0^{2\pi} -F'(r) \frac{\mathbf{r} \cdot \nu(\tau)}{r}\, \psi(\tau)\, d\tau = \int_0^{2\pi} H(t,\tau)\psi(\tau) d\tau \ . \tag{39}$$

We decompose $H(t,\tau)$ as $H(t,\tau) = H_1(t,\tau) \log r^2 + H_2(t,\tau)$, where

$$H_1(t,\tau) = k\, J_1(kr)\, \frac{\mathbf{r} \cdot \nu(\tau)}{4\pi\, r^2} \quad , \quad H_2(t,\tau) = H(t,\tau) - H_1(t,\tau) \log r^2 \ . \tag{40}$$

Here, we have $H_1(t,t) = H_2(t,t) = 0$.

Finally, we parametrize $[(N_k - N_0)\phi](x(t))$ using (8) as

$$[(N_k - N_0)\phi](x(t)) = \frac{1}{|x'(t)|} \int_0^{2\pi} L(t,\tau)\psi(\tau) d\tau + \frac{1}{|x'(t)|} \int_0^{2\pi} M(t,\tau)\psi(\tau) d\tau \ . \tag{41}$$

The kernel M is given by $M(t,\tau) = k^2\nu(t)\cdot\nu(\tau)F(r) = M_1(t,\tau)\log r^2 + M_2(t,\tau)$, where

$$M_1(t,\tau) = \frac{k^2\nu(t)\cdot\nu(\tau)}{4\pi}(1 - J_0(kr)) \quad , \quad M_2(t,\tau) = M(t,\tau) - M_1(t,\tau)\log r^2 \ . \tag{42}$$

The diagonal terms are $M_1(t,t) = 0$ and $M_2(t,t) = \frac{k^2}{2}\left(\frac{i}{2} - \frac{\gamma+\log(k/2)}{\pi}\right)|x'(t)|^2$. The kernel L is given by

$$L(t,\tau) = (F'(r) - F''(r))\frac{\mathbf{r}\cdot x'(t)}{r}\frac{\mathbf{r}\cdot x'(\tau)}{r} - F'(r)\frac{x'(t)\cdot x'(\tau)}{r} \ . \tag{43}$$

As before, we decompose L as $L(t,\tau) = L_1(t,\tau)\log r^2 + L_2(t,\tau)$, where

$$L_1(t,\tau) = \frac{k}{4\pi}\left(J_1(k\,r) - kJ_0(k\,r) + \frac{J_1(k\,r)}{r}\right)\frac{\mathbf{r}\cdot x'(t)}{r}\frac{\mathbf{r}\cdot x'(\tau)}{r} - \frac{kJ_1(k\,r)}{4\pi r}\,x'(t)\cdot x'(\tau) \ , \tag{44}$$

and $L_2(t,\tau) = L(t,\tau) - L_1(t,\tau)\log r^2$. The diagonal terms are $L_1(t,t) = -\frac{k^2}{4\pi}|x'(t)|^2$ and $L_2(t,t) = \frac{k^2}{2}\left(\frac{i}{2} - \frac{\gamma+\log(k/2)+1/2}{\pi}\right)|x'(t)|^2$.

Letting $\psi(t) = u(x(t))$ and $g(t)$ be the parametrization of the right-hand side in (14), we express the integral equation (14) for CFIE-R(0,1) parametrically as

$$g(t) = \left(\frac{1}{2} + \frac{i\eta}{4}\right)\psi(t) + \left(\frac{1}{2} - \frac{i\eta}{4}\right)\psi(0) - \int_0^{2\pi} H(t,\tau)\psi(\tau)\,d\tau \tag{45}$$

$$- \int_0^{2\pi} H_0(t,\tau)(\psi(\tau) - \psi(0))\,d\tau - \frac{i\eta}{2}\int_0^{2\pi} H_0(0,\tau)(\psi(\tau) - \psi(0))\,d\tau \tag{46}$$

$$- i\eta\int_0^{2\pi}\frac{M_0(t,\tau)}{|x'(\tau)|}\left(\int_0^{2\pi}(L(\tau,z) + M(\tau,z))\psi(z)\,dz\right)d\tau \tag{47}$$

$$- i\eta\int_0^{2\pi} H_0(t,\tau)\left(\int_0^{2\pi}(H_0(\tau,z) - H_0(0,z))(\psi(z) - \psi(0))\,dz\right)d\tau \ . \tag{48}$$

More specifically, g is given by

$$g(t) = u^i(x(t)) + i\eta\int_0^{2\pi} M_0(t,\tau)\frac{\partial u^i}{\partial\nu}(x(\tau))\,d\tau \ . \tag{49}$$

3.2 The Quadrature Rules

As we saw above, each of our integral kernels has the generic form $K(t,\tau) = K_1(t,\tau)\log r^2 + K_2(t,\tau)$, where K_j is smooth on $(0,2\pi)\times(0,2\pi)$; and our densities, $\mu(t) = \psi(t) - \psi(0)$ or $\mu(t) = \psi(t)$, can be thought of as generic Hölder functions, whose Hölder-exponent is determined by the angle at the corner, as indicated in Section 2. For a fixed t, then, we have two types of integrals for which we must develop high-order quadratures: those which are smooth in $(0,2\pi)$ but have singular derivatives at the endpoints, and those which additionally have a logarithmic singularity at t. To handle both integrals we will use a combination of a graded-mesh quadrature introduced by Kress [28], which is affected by a suitable change-of-variables, and a quadrature due to Martensen [18, 32] which incorporates certain types of periodic, logarithmic singularities into its quadrature weights. Both quadratures have been analyzed in the cited references, and were designed to yield high-order quadrature rules in precisely the contexts in which we will use them, so here we merely describe

these quadratures in enough detail to be able to implement our method without need for outside reference.

We begin with the change-of-variables $t = w(s)$ where

$$\begin{aligned} w(s) &= 2\pi \frac{[v(s)]^p}{[v(s)]^p + [v(2\pi - s)]^p}, \ 0 \le s \le 2\pi \\ v(s) &= \left(\frac{1}{p} - \frac{1}{2}\right)\left(\frac{\pi - s}{\pi}\right)^3 + \frac{1}{p}\frac{s-\pi}{\pi} + \frac{1}{2} \end{aligned} \tag{50}$$

where $p \ge 2$. The function w is a smooth, increasing, bijection on $[0, 2\pi]$, with $w^{(k)}(0) = w^{(k)}(2\pi) = 0$ for $1 \le k \le p-1$. Using this change-of-variables, we further decompose K as

$$K(t,\tau) = K(w(s), w(\sigma)) = K_1(w(s), w(\sigma)) \log\left(4\sin^2\frac{s-\sigma}{2}\right) + \tilde{K}_2(s,\sigma) \ . \tag{51}$$

We have

$$\tilde{K}_2(s,\sigma) = K(w(s), w(\sigma)) - K_1(w(s), w(\sigma)) \log\left(4\sin^2\frac{s-\sigma}{2}\right) \tag{52}$$

$$= K_1(w(s), w(\sigma)) \log\left(\frac{r^2(w(s), w(\sigma))}{4\sin^2\frac{s-\sigma}{2}}\right) + K_2(w(s), w(\sigma)) \ , \tag{53}$$

with diagonal term $\tilde{K}_2(s,s) = 2K_1(t,t)\log(w'(s)|x'(t)|) + K_2(t,t)$. With this further decomposition, we see that we need quadratures for integrals of the forms $\int_0^{2\pi} f(\sigma)\, d\sigma$ and $\int_0^{2\pi} f(\sigma) \log\left(4\sin^2\frac{s-\sigma}{2}\right) d\sigma$, where f is smooth in $(0, 2\pi)$ and 2π-periodic in its values and a few of its derivatives. The quadratures are of the forms:

$$\int_0^{2\pi} f(\sigma)\, d\sigma \approx \frac{\pi}{n} \sum_{j=0}^{2n-1} f(s_j) \quad \text{and} \quad \int_0^{2\pi} f(\sigma) \log\left(4\sin^2\frac{s-\sigma}{2}\right) d\sigma \approx \sum_{j=0}^{2n-1} R_j^{(n)}(s) f(s_j) \tag{54}$$

for $0 \le s \le 2\pi$, where $s_j = j\pi/n$ and the weights $R_j(s)$ are given by

$$R_j(s) = -\frac{2\pi}{n} \sum_{m=1}^{n-1} \frac{1}{m} \cos m(s - s_j) - \frac{\pi}{n^2} \cos n(s - s_j). \tag{55}$$

We note that $R_j(s_i) = R_{|i-j|}$, where

$$R_k = -\frac{2\pi}{n} \sum_{m=1}^{n-1} \frac{1}{m} \cos\frac{mk\pi}{n} - \frac{(-1)^k \pi}{n^2} \ .$$

We are now ready to express the quadrature for $\int_0^{2\pi} K(t,\tau)\mu(\tau)\, d\tau$ at points $t = t_i = w(s_i)$, namely:

$$\int_0^{2\pi} K(t_i,\tau)\mu(\tau)\, d\tau \approx \sum_{j=1}^{2n-1} (K_1(t_i,t_j)W_{ij} + K_2(t_i,t_j)w_j)\mu(t_j) \ , \tag{56}$$

where the weights are given by

$$W_{ij} = \left(R_{|i-j|} + \frac{\pi}{n}\log\left(\frac{r^2(t_i,t_j)}{4\sin^2\frac{s_i - s_j}{2}}\right)\right) w'(s_j) \quad \text{and} \quad w_j = \frac{\pi}{n}\, w'(s_j) \ . \tag{57}$$

We note that the sum in (56) begins at $j = 1$ instead of $j = 0$ because $W_{i0} = w_0 = 0$. As suggested above, we have $W_{ii} = \left(R_0 + \frac{2\pi}{n} \log(w'(s_i)|x'(t_i)|)\right) w'(s_i)$ for $i > 0$.

3.3 The Nyström Linear System

The Nyström discretization of (45)-(49) is

$$G_m = \left(\frac{1}{2}+\frac{i\eta}{4}\right)u_m^{(n)} + \left(\frac{1}{2}-\frac{i\eta}{4}\right)u_0^{(n)} - \sum_{j=1}^{2n-1}(H_1(t_m,t_j)W_{mj} + H_2(t_m,t_j)w_j)u_j^{(n)} \tag{58}$$

$$- \sum_{j=1}^{2n-1}\left(H_0(t_m,t_j) - \frac{i\eta}{2}H_0(0,t_j)\right)w_j(u_j^{(n)} - u_0^{(n)}) \tag{59}$$

$$- i\eta\sum_{j=1}^{2n-1}\left(\frac{M_{01}(t_m,t_j)}{|x'(t_j)|}W_{mj} + \frac{M_{02}(t_m,t_j)}{|x'(t_j)|}w_j\right)\sum_{k=1}^{2n-1}(L_1(t_j,t_k)W_{jk} + L_2(t_j,t_k)w_k)u_k^{(n)} \tag{60}$$

$$- i\eta\sum_{j=1}^{2n-1}\left(\frac{M_{01}(t_m,t_j)}{|x'(t_j)|}W_{mj} + \frac{M_{02}(t_m,t_j)}{|x'(t_j)|}w_j\right)\sum_{k=1}^{2n-1}(M_1(t_j,t_k)W_{jk} + M_2(t_j,t_k)w_k)u_k^{(n)} \tag{61}$$

$$- i\eta\sum_{j=1}^{2n-1}H_0(t_m,t_j)w_j\left(\sum_{k=1}^{2n-1}(H_0(t_j,t_k) - H_0(0,t_k))w_k(u_k^{(n)} - u_0^{(n)})\ .\right) \tag{62}$$

Here we have $u_m^{(n)} \approx u(x(t_m))$, and load vector $\mathbf{G}$ given by

$$G_m = u^i(x(t_m)) + i\eta\sum_{j=0}^{2n-1}(M_{01}(t_m,t_j)W_{mj} + M_{02}(t_m,t_j)w_j)\frac{\partial u^i}{\partial \nu}(x(t_j)). \tag{63}$$

Discretizations of the integral equation formulations DCFIE-R(0,2) and DCFIE-R(1,1) can be obtained in a similar manner. The discretization of DCFIE-RC formulations, on the other hand, involves modifications of the quadrature rules presented above to the case of boundary layers corresponding to purely imaginary wave numbers. For instance, following [8], the single layer potentials related to wave numbers iK are expressed as

$$(S_{iK}\phi)(x(t)) = \int_0^{2\pi}\hat{M}(t,\tau)|x'(\tau)|\phi(x(\tau))d\tau \tag{64}$$

we use the following splitting of the kernel $\hat{M}(t,\tau) = \frac{i}{4}H_0^{(1)}(iKr)$:

$$\hat{M}(t,\tau) = e^{-Kr^4}\left\{\hat{M}_1(t,\tau)\ln\left(4\sin^2\frac{t-\tau}{2}\right) + \hat{M}_2(t,\tau)\right\} + (1-e^{-Kr^4})\hat{M}(t,\tau) \tag{65}$$

with $\hat{M}_1(t,\tau) = -\frac{1}{4\pi}J_0(iKr)$; each of the terms in the splitting above is amenable to the same quadrature rules as the ones developed for the kernels with real wave numbers. This splitting procedure allows to treat the operators K_{iK} and N_{iK} in a similar manner.

4 Numerical Results

We present in this section a variety of numerical results that demonstrate the properties of the regularized combined field integral equations (14) constructed in the previous sections. Solutions of the linear systems (58)-(63) are obtained by means of the fully complex version of the iterative

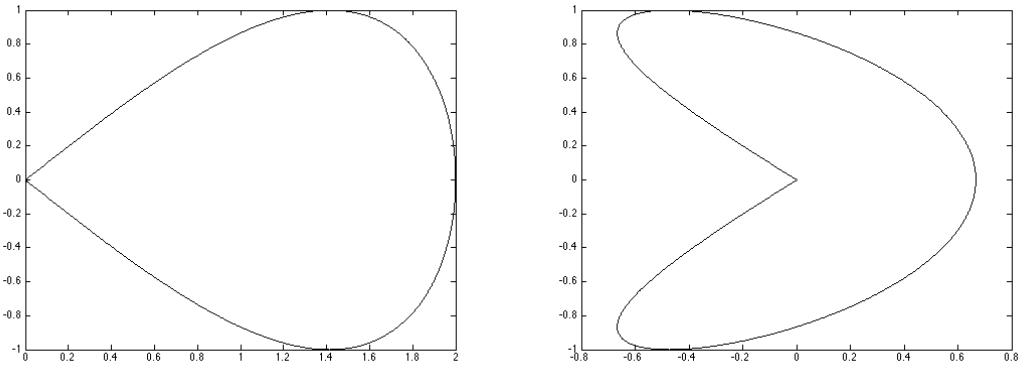

Figure 1: Teardrop (left) and boomerang (right), $\alpha = 1/2$.

solver GMRES [39]. The first set of results presented concern the various DCFIE-R formulations that use the regularizing operators of the form S_0^d, and the second set of the results concern the DCFIE-RC(0,1) formulation that uses the regularizing operators of the form S_{iK} with $K > 0$. Of the three possible formulations (14) stemming from the use of the regularizing operators S_0^d, DCFIE-R(0,1) entails (i) the smallest computational time as it involves only two compositions of operators, and (ii) the smallest condition numbers. For the formulation DCFIE-R(0,1) we used coupling parameters $\eta = 1/k$ for the results in Tables 1, 4, 5, 6, and $\eta = 8/k$ for the results in Table 2. Although the statement of Theorem 2.5 requires that a "sufficiently small" coupling parameter η should be used in DCFIE-R(0,1), we have found in practice that a fairly wide range of coupling parameters, including the aforementioned choice, leads to integral operators whose discrete approximations have spectra bounded away from 0 (see Figure 2 for an illustration of the effect of the coupling parameter η on the conditioning numbers of the various formulations). Furthermore, we have found that these choices of the coupling parameter yield good behavior of the iterative solvers. We also used the same coupling parameter $\eta = 1/k$ for the other formulations DCFIE-R(1,1) and DCFIE-R(0,2). Most of the results contained in the tables presented in this section were obtained by prescribing a GMRES residual tolerance equal to 10^{-8}; otherwise, we used a GMRES residual tolerance equal to 10^{-12}.

We will show results for two geometries, having convex and concave corners: the teardrop domain, with boundary parametrized by $x(t) = (2\sin\frac{t}{2}, -\beta\sin t)$; and the boomerang domain, with boundary parametrized by $x(t) = (-\frac{2}{3}\sin\frac{3t}{2}, -\beta\sin t)$. Here $\beta = \tan\frac{\alpha\pi}{2}$, and $\alpha\pi$ is the acute aperture of the corner (see Figure 1). For these configurations the diameter of the corresponding domains D is equal to 2, and we chose $d = 4$ in the definition of the regularizing operators S_0^d. For every scattering experiment we present:

- the maximum error incurrent in the total field u on Γ defined as

$$E_1 = \max_{0\le j\le 2n-1} |u_j^{(n)} - u_{qj}^{\text{ref}}| \tag{66}$$

  where the reference solution u^{ref} corresponds to a very refined discretization corresponding to $2qn$ discretization points, and

- the maximum error amongst several directions $\hat{\mathbf{x}} = \frac{\mathbf{x}}{|\mathbf{x}|}$ in the far-field pattern $u_\infty^s(\hat{\mathbf{x}})$,

$$E_2 = \max|u_\infty^{s,\text{calc}}(\hat{\mathbf{x}}) - u_\infty^{s,\text{ref}}(\hat{\mathbf{x}})| \tag{67}$$

where the maximum is taken over a uniform discretization of the unit circle $|\hat{\mathbf{x}}| = 1$ comprised of 256 points. The (exact) far-field pattern is defined by the relation

$$u^s(\mathbf{x}) = \frac{e^{ik|\mathbf{x}|}}{\sqrt{|\mathbf{x}|}} \left(u^s_\infty(\hat{\mathbf{x}}) + \mathcal{O}\left(\frac{1}{|\mathbf{x}|}\right)\right), \ |\mathbf{x}| \to \infty \ . \tag{68}$$

Once the solution $u^{(n)}$ of the linear system (58)-(63) is produced, the far-field can be obtained immediately from equation (11)

$$u^{s,\text{calc}}_\infty(\hat{x}) = \frac{e^{-\frac{i\pi}{4}}}{n\sqrt{8}}\sqrt{k\pi} \sum_{j=1}^{2n-1} \hat{x}\cdot\nu(t_j) e^{-ik\hat{x}\cdot x(t_j)} u^{(n)}_j w'(s_j) \ . \tag{69}$$

The maximum far-field error is evaluated through comparison of the numerical solutions $u^{s,\text{calc}}_\infty$ with reference solutions $u^{s,\text{ref}}_\infty$—solutions obtained from very fine discretizations in the case of plane wave incidences, and exact solutions in the case of point-source incidences.

For plane wave incidences, the reference solutions arising from very fine discretizations were produced through an LU solution of the linear system (58)-(63) obtained from the discretization of the formulation DCFIE-R(0,1). We also present in Table 2 the far-field errors between the reference solutions obtained using very refined discretizations of formulations DCFIE-R(0,1) and the ones obtained from the same discretizations with formulations DCFIE-R(1,1) and DCFIE-R(0,2). Besides errors in the total field u on the boundary of the scatterer and the far field errors, the tables display the number of iterations required by the GMRES solver to a relative residual of 10^{-8}; or of 10^{-12}, if denoted by $*$. We used discretizations corresponding to 8 and 16 points per wavelength, for frequencies in the medium to high-frequency range, i.e. $k = 2^i, i = 3, \ldots, 8$ corresponding to acoustic scattering problems of sizes ranging from 2.5λ to 81.6λ. In the range $k = 2^i, i = 3, \ldots, 8$ the reference solutions were obtained using 24 points per wavelength. In the low frequency regime, i.e $k = 1, 4$ the reference solutions were obtained using $n = 128$, that is 256 unknowns, in equations (58)-(63). For the case of plane-wave incidence we assumed an incident field in the form of a plane wave propagating along the x axis, i.e. its direction of propagation is $d = (1, 0)$. In all of the numerical examples we used $p = 8$ in the change of variables (50) for the teardrop geometry and $p = 4$ for the boomerang geometry. The reason for using different values of p is that the solutions u of (14) can be shown to be in the Hölder space $C^{0,\frac{2}{3}}(\Gamma)$ for the boomerang geometry and $C^1(\Gamma)$ for the case of the boomerang, and thus a higher exponent is needed in the change of variables (50) to resolve the stronger singularity of u in the first case.

We start by presenting numerical results for plane-wave incidence Tables 1-4 for the domains with interior/exterior apertures of $\pi/2$. As it can be seen, our solutions converge to high order throughout a wide range of frequencies. Furthermore, the reference solutions exhibit very high accuracy regardless of the formulation used. We note that similar numbers of GMRES iterations are required if the same formulation (14) were used for smooth curves [8].

The computational times entailed by a matrix-vector product for each of the three formulations DCFIE-R are close to each other, owing to the fact that the evaluation of the operator S^d_0 is fairly inexpensive relative to all of the other acoustic integral operators involved in the DCFIE-R formulations. Nevertheless, the formulation DCFIE-R(0,1) is slightly less expensive than the other two formulations since it involves only two operator compositions. We illustrate in Table 3 the computational times required to build the matrix according to equations (58)-(63) and its analogues in each of the three DCFIE-R formulations (the computational times are about the

Table 1: Plane wave incidence, geometries with interior/exterior apertures of $\pi/2$

k	Unknowns	Teardrop $\alpha = 1/2$			Boomerang $\alpha = 1/2$		
		Iter.	E_1	E_2	Iter.	E_1	E_2
1	32	12	7.6×10^{-6}	6.2×10^{-7}	13	9.7×10^{-4}	2.3×10^{-4}
1	64	11	5.1×10^{-8}	2.6×10^{-10}	15	6.1×10^{-7}	4.8×10^{-8}
1	128	10	4.2×10^{-10}	7.5×10^{-12}	13	2.3×10^{-8}	1.4×10^{-10}
4	32	13	8.4×10^{-3}	4.2×10^{-3}	16	3.0×10^{-1}	1.8×10^{-1}
4	64	13	3.1×10^{-6}	4.9×10^{-8}	17	3.3×10^{-5}	1.3×10^{-7}
4	128	13	1.5×10^{-8}	5.7×10^{-10}	15	3.4×10^{-7}	8.6×10^{-10}
8	64	17	2.7×10^{-3}	9.7×10^{-4}	21	4.9×10^{-3}	1.5×10^{-3}
8	128	17	6.9×10^{-9}	3.9×10^{-10}	19	2.1×10^{-6}	2.1×10^{-9}
16	128	27	7.0×10^{-4}	2.4×10^{-4}	29	2.8×10^{-3}	1.6×10^{-3}
16	256	25	5.3×10^{-9}	5.3×10^{-10}	26	2.4×10^{-7}	1.3×10^{-8}
32	256	40	5.3×10^{-4}	2.7×10^{-4}	42	9.8×10^{-4}	4.5×10^{-4}
32	512	40	1.9×10^{-8}	3.5×10^{-9}	41	4.2×10^{-8}	4.0×10^{-9}

Table 2: Comparisons reference solutions, geometries with interior/exterior apertures of $\pi/2$

k	Unknowns	Teardrop $\alpha = 1/2$		Boomerang $\alpha = 1/2$	
		DCFIE-R(0,2) E_2	DCFIE-R(1,1)E_2	DCFIE-R(0,2)E_2	DCFIE-R(1,1)E_2
1	256	1.9×10^{-15}	3.3×10^{-14}	9.7×10^{-14}	8.5×10^{-14}
4	256	3.4×10^{-15}	3.9×10^{-15}	4.2×10^{-13}	5.3×10^{-13}
8	256	6.3×10^{-15}	5.6×10^{-15}	4.9×10^{-13}	7.8×10^{-13}
16	512	1.5×10^{-14}	2.3×10^{-14}	3.5×10^{-14}	3.7×10^{-14}
32	1024	7.8×10^{-14}	5.6×10^{-14}	1.0×10^{-13}	9.9×10^{-14}

Table 3: Computational times needed by the various formulations

Unknowns	Times		
	DCFIE-R(0,1)	DCFIE-R(0,2)	DCFIE-R(1,1)
64	1.13 sec	1.15 sec	1.16 sec
128	3.72 sec	3.74 sec	3.74 sec
256	14.75 sec	14.79 sec	14.82 sec

Table 4: Plane wave incidence, higher frequencies, geometries with interior/exterior apertures of $\pi/2$

k	Unknowns	Teardrop $\alpha = 1/2$			Boomerang $\alpha = 1/2$		
		Iter.	E_1	E_2	Iter.	E_1	E_2
64	512	48	2.0×10^{-4}	1.1×10^{-4}	54	3.6×10^{-4}	1.4×10^{-4}
64	1024	48	7.2×10^{-9}	1.3×10^{-9}	54	1.4×10^{-7}	3.0×10^{-8}
128	1024	80	8.9×10^{-5}	2.0×10^{-5}	94	4.8×10^{-5}	3.1×10^{-5}
128	2048	80	2.7×10^{-7}	6.5×10^{-9}	94	2.1×10^{-7}	1.8×10^{-8}
256	2048	136	2.1×10^{-5}	1.1×10^{-5}	167	2.3×10^{-5}	5.8×10^{-6}
256	4096	136	2.1×10^{-7}	2.3×10^{-9}	167	2.1×10^{-7}	3.0×10^{-9}

same for each of the geometries under consideration). The computational times resulted from a MATLAB implementation of our solver on a MacPro machine with 2 × 3GHz Quad-core Intel Xeon. The computational times reported are only 1.2 times more expensive than those required for the corresponding solvers for smooth geometries [8].

The formulation DCFIE-R gives rise to smaller condition numbers upon discretizations, as illustrated in Figure 2. We present in Figure 2 the condition numbers of the three DCFIE-R as functions of the coupling parameter η for five wave numbers $k = 1, 4, 8, 16, 32$ using 128 unknowns in each case, for the domains considered above with $\alpha = 1/2$. Specifically, for each wave number and geometry we considered 32 coupling parameters $\eta = i/(8k), i = 1, 2 \ldots, 32$ as this range of values of η was found to lead to lower condition numbers. The second conclusion that can be drawn from the results in Figure 2 is that the DCFIE-R(0,1) formulation is well-conditioned in that given range of coupling parameters η.

The next set of results in Table 5 illustrates the high-order convergence of our algorithm using the formulation DCFIE-R(0,1) for singular geometries with more acute interior/exterior corners, i.e. $\alpha = 1/6$ in the definition of the teardrop and boomerang domains.

In order to further confirm the high-order accuracy of our solvers, we present in the next set of numerical experiments Tables 6-7 results obtained in cases when radiative point-source incident fields with sources inside the obstacle were used as incident fields. Specifically, we assumed the point-source to be located inside the scatterers close to the corner at $(0.1, 0)$. In these cases, the solution of the exterior Neumann problem is the point-source itself which allows for a direct evaluation of the far-field errors. For such incident fields, the left-hand side of equation (10) needs be replaced by u^i and thus equations DCFIE-R(0,1) (14) should be modified so that the coefficient of the double layer operator K_k is 1 rather than -1. Again, the high-order convergence of our algorithm is demonstrated by the results in Table 6-7.

In the next set of the results we present the number of iterations and condition numbers that

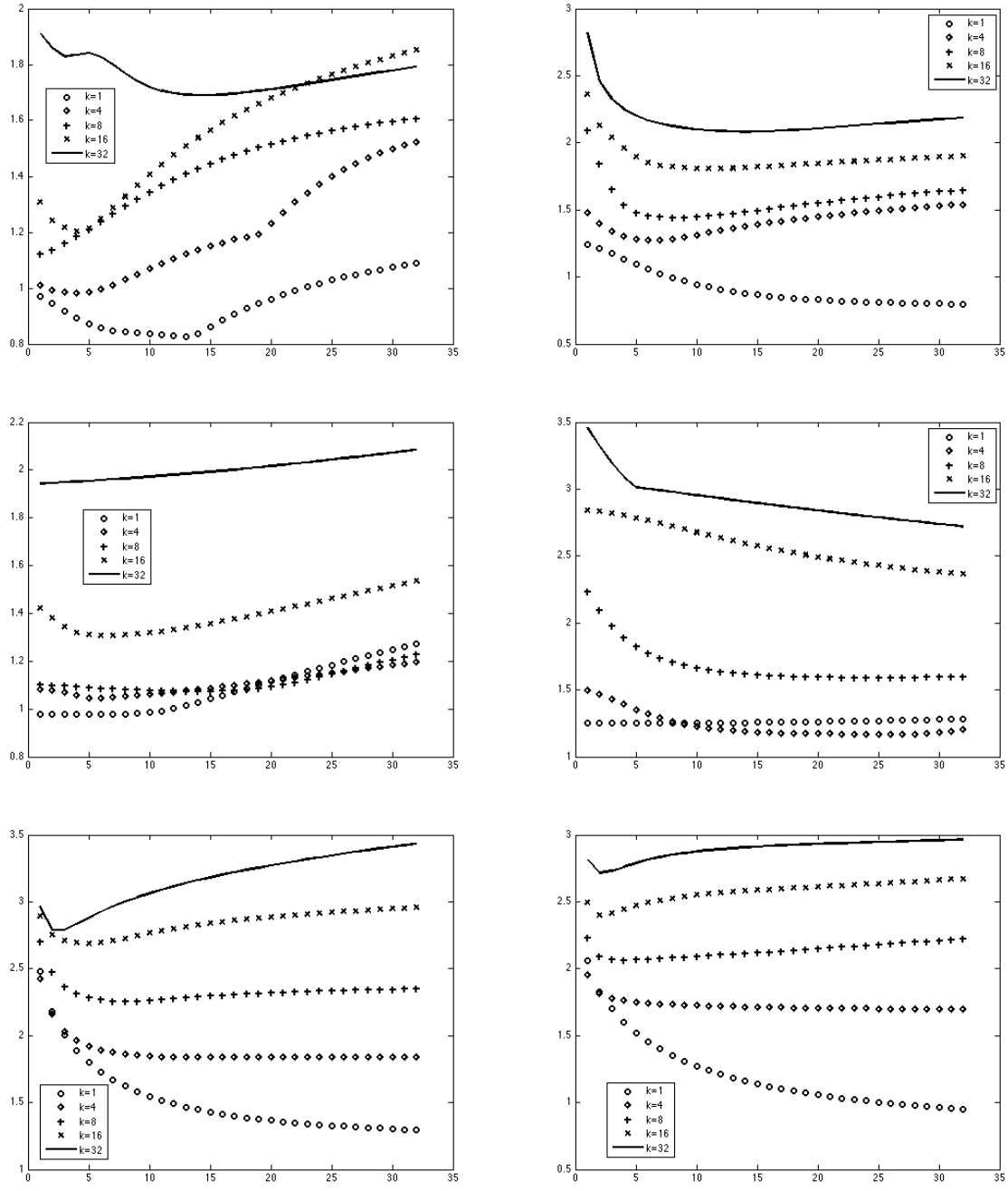

Figure 2: Plots of the decimal logarithms of the condition numbers of the discretizions of the formulations DCFIE-R(0,1) (top), DCFIE-R(1,1) (middle), and DCFIE-R(0,2) (bottom) as functions of the wave number k and the coupling parameter η for the teardrop (left) and boomerang (right) geometries with $\alpha = 1/2$. The results shown correspond to problems with 128 unknowns, and wave numbers $k = 1, 4, 8, 16, 32$ and 32 coupling parameters for each formulation: $\eta = j/(8k)$, $j = 1, 2 \ldots, 32$.

Table 5: Plane wave incidence, geometries with interior/exterior apertures of $\pi/6$

k	Unknowns	Teardrop			Boomerang		
		Iter.	E_1	E_2	Iter.	E_1	E_2
1	32	15	4.2×10^{-3}	2.8×10^{-4}	19	5.2×10^{-1}	2.3×10^{-3}
1	64	15	1.5×10^{-4}	3.4×10^{-6}	22	6.8×10^{-3}	1.2×10^{-4}
1	128	14	1.5×10^{-6}	6.0×10^{-9}	23	4.1×10^{-5}	2.3×10^{-7}
1	256	11	2.7×10^{-8}	3.2×10^{-11}	24	2.2×10^{-6}	2.7×10^{-9}
4	32	17	1.4×10^{-2}	2.6×10^{-3}	19	1.1×10^{0}	3.4×10^{-2}
4	64	17	4.8×10^{-4}	2.6×10^{-5}	25	2.3×10^{-2}	2.6×10^{-4}
4	128	16	4.4×10^{-6}	4.5×10^{-8}	27	4.1×10^{-5}	6.4×10^{-7}
4	256	13	1.7×10^{-8}	4.2×10^{-11}	29	1.5×10^{-6}	2.2×10^{-9}
8	64	21	1.1×10^{-3}	2.4×10^{-4}	28	7.0×10^{-2}	7.7×10^{-4}
8	128	20	9.3×10^{-6}	3.0×10^{-7}	30	3.4×10^{-5}	6.3×10^{-7}
8	256	18	2.7×10^{-8}	9.4×10^{-11}	32	1.5×10^{-6}	3.0×10^{-9}
16	128	27	9.6×10^{-5}	2.2×10^{-5}	34	4.3×10^{-4}	3.3×10^{-5}
16	256	24	5.0×10^{-8}	7.0×10^{-10}	36	1.9×10^{-6}	2.6×10^{-8}
32	256	38	1.4×10^{-5}	3.2×10^{-7}	49	8.1×10^{-5}	7.6×10^{-6}
32	512	35	1.6×10^{-7}	2.6×10^{-9}	51	1.9×10^{-7}	4.5×10^{-9}

Table 6: Point source incidence geometries with interior/exterior apertures of $\pi/2$

k	Unknowns	Teardrop		Boomerang	
		Iter.	E_2	Iter.	E_2
1	32	16	6.9×10^{-3}	12	4.4×10^{-5}
1	64	14	5.3×10^{-5}	13	2.3×10^{-8}
1	128	14	2.4×10^{-9}	12	1.1×10^{-10}
1	256	19^*	3.3×10^{-15}	16^*	8.9×10^{-15}
4	32	18	4.0×10^{-3}	14	1.9×10^{-4}
4	64	18	3.0×10^{-5}	14	3.1×10^{-7}
4	128	18	1.3×10^{-9}	15	2.1×10^{-10}
4	256	24^*	2.0×10^{-14}	19^*	4.3×10^{-14}
8	64	24	4.0×10^{-5}	19	1.6×10^{-4}
8	128	22	1.9×10^{-9}	19	1.0×10^{-10}
16	128	32	2.4×10^{-5}	27	2.0×10^{-4}
16	256	30	9.6×10^{-11}	26	1.3×10^{-9}
32	256	46	5.7×10^{-5}	43	3.5×10^{-5}
32	512	46	6.3×10^{-10}	43	9.8×10^{-11}

Table 7: Point source incidence geometries with interior/exterior apertures of $\pi/6$

k	Unknowns	Teardrop		Boomerang	
		Iter.	E_2	Iter.	E_2
1	32	21	5.0×10^{-2}	17	4.9×10^{-3}
1	64	31	9.6×10^{-3}	19	1.4×10^{-4}
1	128	37	2.7×10^{-4}	19	1.2×10^{-7}
1	256	36	3.4×10^{-7}	19	2.2×10^{-10}
1	512	44*	2.2×10^{-13}	27*	1.2×10^{-14}
4	32	22	2.1×10^{-2}	17	3.2×10^{-3}
4	64	34	4.8×10^{-3}	18	1.0×10^{-4}
4	128	41	1.3×10^{-4}	18	7.9×10^{-8}
4	256	42	1.7×10^{-7}	18	1.9×10^{-10}
4	512	50*	1.1×10^{-13}	27*	3.8×10^{-15}
8	64	34	2.8×10^{-3}	20	2.0×10^{-4}
8	128	44	8.1×10^{-5}	20	1.1×10^{-7}
8	256	44	1.1×10^{-7}	20	9.7×10^{-11}
16	128	58	7.5×10^{-5}	26	1.3×10^{-6}
16	256	58	5.0×10^{-8}	25	8.5×10^{-11}
16	512	58	3.6×10^{-10}	34*	1.6×10^{-14}
32	256	77	3.5×10^{-8}	37	1.5×10^{-7}
32	512	62	3.4×10^{-10}	37	5.8×10^{-10}

result from the implementation of DCFIE-RC(0,1) that uses $S_{ik/2}$ for regularizing operators. As can be seen from the results in Table 8, these formulations result in significantly smaller numbers of iterations—especially for higher frequencies when the gains in numbers of iterations are of order three—to the same GMRES residuals that their DCFIE-R(0,1) counterparts that use S_0^d as regularizing operators. Furthermore, the accuracy levels achieved by the DCFIE-RC(0,1) formulation using $S_{ik/2}$ are comparable to those corresponding to the same formulations but using S_0^d. Given that a matrix-vector products in the former formulation is about 1.6 more expensive that its counterpart in the latter formulation, computational gains of about a factor of two can be garnered from the use of $S_{ik/2}$ in the DCFIE-RC(0,1) formulations for higher frequencies when iterative solvers are used. The larger computational times required by a matrix-vector product corresponding to the DCFIE-RC(0,1) formulation is related to the larger computational times required by the evaluation of the layer potentials N_{iK}, S_{iK}, and K_{iK} in equation (34) with respect to their counterparts N_0, S_0, and K_0 in equation (33).

In order to illustrate further the superior conditioning properties of the DCFIE-RC(0,1) formulations, we present in Figure 3 the decimal logarithms of the condition numbers resulting from the implementation of this formulation for the boomerang geometries for the same wave numbers as in Figure 2 and coupling parameters $\eta = i/16, i = 1, 2 \ldots, 32$. Consistent with the results in Table 8, the DCFIE-RC(0,1) formulations give rise to smaller condition numbers than those entailed by the formulation DCFIE-R(0,1). For the convex teardrop geometries, the condition numbers vary very slowly as functions of the wave numbers for coupling parameters η in the range from 1 to 2: for the case $\alpha = 1/2$ the decimal logarithms of the condition numbers are about 0.94 whereas those for the case $\alpha = 1/6$ are around 1.5.

Table 8: Number of iterations using DCFIE-RC(0,1) with $S_{ik/2}$, $\eta = 1$, plane wave incidence, GMRES residual 10^{-8}.

k	Unknowns	Teardrop Iter.		Boomerang Iter.	
		$\alpha = 1/2.$	$\alpha = 1/6$	$\alpha = 1/2$	$\alpha = 1/6$
1	64	10	12	13	22
4	64	14	14	15	24
8	64	16	15	19	25
16	128	17	16	22	31
32	256	20	22	24	41
64	512	21	22	26	47
128	1024	25	26	27	53
256	2048	29	26	32	54

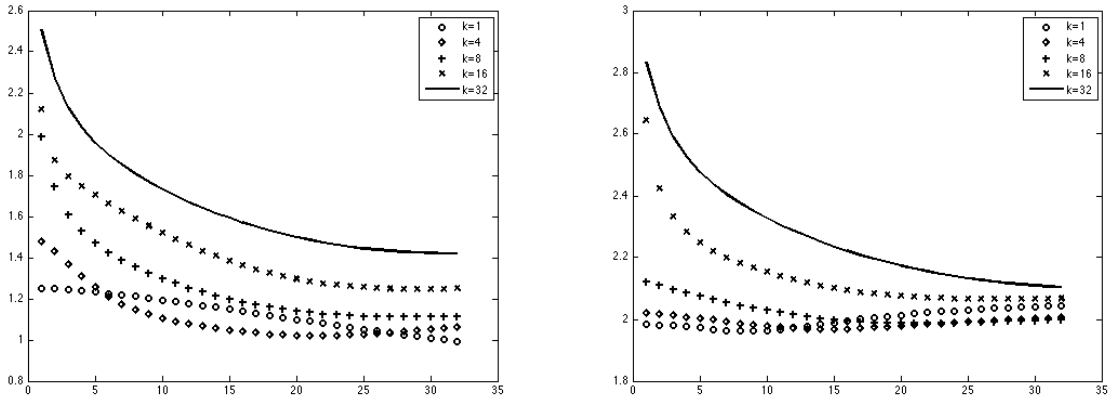

Figure 3: Plots of the decimal logarithms of the condition numbers of the discretizions of the formulations DCFIE-RC(0,1) using the regularizing operators $S_{ik/2}$ as functions of the wave number k and the coupling parameter η for the boomerang geometries with $\alpha = 1/2$ (left) and $\alpha = 1/6$ (right). The results shown correspond to problems having 128 unknowns, and wave numbers $k = 1, 4, 8, 16, 32$ and 32 coupling parameters for each formulation: $\eta = j/16$, $j = 1, 2 \ldots, 32$.

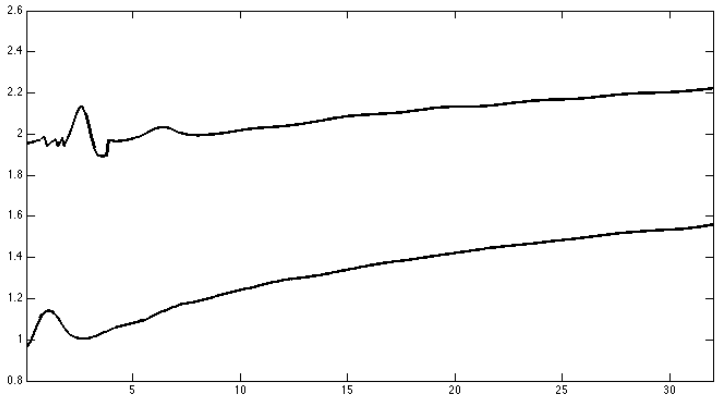

Figure 4: Plots of the decimal logarithms of the condition numbers of the discretizions of the formulations DCFIE-RC(0,1) using the regularizing operators $S_{ik/2}$ and $\eta = 1$ as functions of the wave number k for the boomerang geometries. We chose 320 wave numbers $k = 0.1, 0.2, \ldots, 32$ and 128 unknown for each case, $p = 4$ in the change of variables formula (50) for each boomerang geometry. The curve on the bottom corresponds to the case $\alpha = 1/2$ and the curve on the top corresponds to the case $\alpha = 1/6$.

Finally, we conclude with an example in Figure 4 that shows the condition numbers of the formulations DCFIE-RC(0,1) as functions of the wave numbers of the incidence radiation. We computed these condition numbers for 320 frequencies in the range $k = 0.1, 0.2, \ldots, 32$ using discretizations involving 128 unknowns, the regularizing operators $S_{ik/2}$, and coupling parameters $\eta = 1$. We plot the conditions numbers for the boomerang geometries: the case $\alpha = 1/2$ is illustrated in the curve on the bottom, and the case $\alpha = 1/6$ by the curve on top. For the case of teardrop geometries, the condition numbers vary slowly with the wave number, the values of the decimal logarithms of the condition numbers are about 0.94 for the case $\alpha = 1/2$ and around 1.5 for the case $\alpha = 1/6$.

In summary, we have found that for low and medium frequencies (i.e. acoustic problems where the size of the scatterer is smaller than 10λ) the formulation DCFIE-R(0,1) with coupling parameter $\eta = 1/k$ leads to rapidly converging solutions. For high frequencies (i.e. acoustic problems where the size of the scatterer is larger than 10λ) the formulation DCFIE-RC(0,1) with regularizing operator $S_{ik/2}$ and coupling parameter $\eta = 1$ possesses excellent spectral properties. Consequently, we advocate the use of these formulations for solutions of sound-hard scattering problems in two-dimensional domains with corners.

5 Conclusions

We presented a class of Direct Regularized Combined Field Integral Equations formulations for the solution of scattering equations with Neumann boundary conditions for domains with corners. These integral equation formulations are well conditioned on account of the choice of the regularizing operators and the high-order approximations of the singular solutions that we used. Highly accurate results for a variety of configurations can be obtained from the use of this formulation throughout a wide range of the acoustic frequency spectrum. Thus, these features make our Direct Regularized Combined Field Integral Equations a viable method of solution to the sound-hard

scattering problems for domains with corners.

References

[1] M. Abramowitz and I. A. Stegun. *Handbook of mathematical functions with formulas, graphs, and mathematical tables*, volume 55 of *National Bureau of Standards Applied Mathematics Series*. For sale by the Superintendent of Documents, U.S. Government Printing Office, Washington, D.C., 1964.

[2] S. Amini and P. J. Harris. A comparison between various boundary integral formulations of the exterior acoustic problem. *Comput. Methods Appl. Mech. Engrg.*, 84(1):59–75, 1990.

[3] A. Anand, O. P. Bruno, J. Ovall, and C. Turc. A high-order integral algorithm for solutions of scattering problems in 3d Lipschitz domains. in preparation, 2009.

[4] X. Antoine and M. Darbas. Alternative integral equations for the iterative solution of acoustic scattering problems. *Quart. J. Mech. Appl. Math.*, 58(1):107–128, 2005.

[5] X. Antoine and M. Darbas. Generalized combined field integral equations for the iterative solution of the three-dimensional Helmholtz equation. *M2AN Math. Model. Numer. Anal.*, 41(1):147–167, 2007.

[6] M. Borsuk and V. Kondratiev. *Elliptic boundary value problems of second order in piecewise smooth domains*, volume 69 of *North-Holland Mathematical Library*. Elsevier Science B.V., Amsterdam, 2006.

[7] O. P. Bruno, T. Elling, R. Paffenroth, and C. Turc. Well-conditioned high-order algorithms for the solution of three-dimensional surface acoustic scattering problems with Neumann boundary conditions. submitted, 2009.

[8] O. P. Bruno, S. Lintner, and C. Turc. Well-conditioned high-order algorithms for the solution of two-dimensional acoustic scattering problems with Neumann boundary conditions. submitted, 2009.

[9] O. P. Bruno, J. S. Ovall, and C. Turc. A high-order integral algorithm for highly singular PDE solutions in Lipschitz domains. *Computing*, 84(3-4):149–181, 2009.

[10] A. Buffa and R. Hiptmair. A coercive combined field integral equation for electromagnetic scattering. *SIAM J. Numer. Anal.*, 42(2):621–640 (electronic), 2004.

[11] A. Buffa and R. Hiptmair. Regularized combined field integral equations. *Numer. Math.*, 100(1):1–19, 2005.

[12] A. J. Burton. Numerical solution of acoustic radiation problems. NPL Contract Report OC5/535, National Physical Laboratory, Teddington, Middlesex, UK, 1976.

[13] A. J. Burton and G. F. Miller. The application of integral equation methods to the numerical solution of some exterior boundary-value problems. *Proc. Roy. Soc. London. Ser. A*, 323:201–210, 1971. A discussion on numerical analysis of partial differential equations (1970).

[14] A. P. Calderón. The multipole expansion of radiation fields. *J. Rational Mech. Anal.*, 3:523–537, 1954.

[15] S. N. Chandler-Wilde and S. Langdon. A Galerkin boundary element method for high frequency scattering by convex polygons. *SIAM J. Numer. Anal.*, 45(2):610–640 (electronic), 2007.

[16] S. H. Christiansen and J.-C. Nédélec. Des préconditionneurs pour la résolution numérique des équations intégrales de frontière de l'électromagnétisme. *C. R. Acad. Sci. Paris Sér. I Math.*, 331(9):733–738, 2000.

[17] R. R. Coifman, A. McIntosh, and Y. Meyer. L'intégrale de Cauchy définit un opérateur borné sur L^2 pour les courbes lipschitziennes. *Ann. of Math. (2)*, 116(2):361–387, 1982.

[18] D. Colton and R. Kress. *Inverse acoustic and electromagnetic scattering theory*, volume 93 of *Applied Mathematical Sciences*. Springer-Verlag, Berlin, second edition, 1998.

[19] D. L. Colton and R. Kress. *Integral equation methods in scattering theory*. Pure and Applied Mathematics (New York). John Wiley & Sons Inc., New York, 1983. A Wiley-Interscience Publication.

[20] M. Costabel. Boundary integral operators on Lipschitz domains: elementary results. *SIAM J. Math. Anal.*, 19(3):613–626, 1988.

[21] M. Costabel and M. Dauge. Singularities of electromagnetic fields in polyhedral domains. *Arch. Ration. Mech. Anal.*, 151(3):221–276, 2000.

[22] M. Costabel and E. Stephan. A direct boundary integral equation method for transmission problems. *J. Math. Anal. Appl.*, 106(2):367–413, 1985.

[23] P. Grisvard. *Elliptic problems in nonsmooth domains*, volume 24 of *Monographs and Studies in Mathematics*. Pitman (Advanced Publishing Program), Boston, MA, 1985.

[24] D. S. Jerison and C. E. Kenig. The Dirichlet problem in nonsmooth domains. *Ann. of Math. (2)*, 113(2):367–382, 1981.

[25] D. S. Jerison and C. E. Kenig. The Neumann problem on Lipschitz domains. *Bull. Amer. Math. Soc. (N.S.)*, 4(2):203–207, 1981.

[26] V. A. Kondratiev. Boundary value problems for elliptic equations in domains with conical or angular points. *Trudy Moskov. Mat. Obšč.*, 16:209–292, 1967.

[27] V. A. Kozlov, V. G. Maz′ya, and J. Rossmann. *Elliptic boundary value problems in domains with point singularities*, volume 52 of *Mathematical Surveys and Monographs*. American Mathematical Society, Providence, RI, 1997.

[28] R. Kress. A Nyström method for boundary integral equations in domains with corners. *Numer. Math.*, 58(2):145–161, 1990.

[29] R. Kress. On the numerical solution of a hypersingular integral equation in scattering theory. *J. Comput. Appl. Math.*, 61(3):345–360, 1995.

[30] R. Kress. *Linear integral equations*, volume 82 of *Applied Mathematical Sciences*. Springer-Verlag, New York, second edition, 1999.

[31] D. P. Levadoux. *Etude d'une équation intégrale adaptaeé à la resolution haute-fréquance de l'equation D'Helmholtz*. PhD thesis, l'Université de Paris VI, France, 2001.

[32] E. Martensen. Über eine Methode zum räumlichen Neumannschen Problem mit einer Anwendung für torusartige Berandungen. *Acta Math.*, 109:75–135, 1963.

[33] A.-W. Maue. Zur Formulierung eines allgemeinen Beugungsproblems durch eine Integralgleichung. *Z. Physik*, 126:601–618, 1949.

[34] W. McLean. *Strongly elliptic systems and boundary integral equations*. Cambridge University Press, Cambridge, 2000.

[35] M. Mitrea. Boundary value problems and Hardy spaces associated to the Helmholtz equation in Lipschitz domains. *J. Math. Anal. Appl.*, 202(3):819–842, 1996.

[36] J.-C. Nédélec and J. Planchard. Une méthode variationnelle d'éléments finis pour la résolution numérique d'un problème extérieur dans R^3. *Rev. Française Automat. Informat. Recherche Opérationnelle Sér. Rouge*, 7(R-3):105–129, 1973.

[37] O. I. Panič. On the solubility of exterior boundary-value problems for the wave equation and for a system of Maxwell's equations. *Uspehi Mat. Nauk*, 20(1 (121)):221–226, 1965.

[38] S. Prössdorf and B. Silbermann. *Numerical analysis for integral and related operator equations*, volume 52 of *Operator Theory: Advances and Applications*. Birkhäuser Verlag, Basel, 1991.

[39] Y. Saad and M. H. Schultz. GMRES: a generalized minimal residual algorithm for solving nonsymmetric linear systems. *SIAM J. Sci. Statist. Comput.*, 7(3):856–869, 1986.

[40] G. Verchota. Layer potentials and regularity for the Dirichlet problem for Laplace's equation in Lipschitz domains. *J. Funct. Anal.*, 59(3):572–611, 1984.

[41] N. M. Wigley. Asymptotic expansions at a corner of solutions of mixed boundary value problems. *J. Math. Mech.*, 13:549–576, 1964.

[42] S. S. Zargaryan and V. G. Maz′ya. The asymptotic form of the solutions of integral equations of potential theory in the neighbourhood of the corner points of a contour. *Prikl. Mat. Mekh.*, 48(1):169–174, 1984.